The Company of Biologists

RESEARCH ARTICLE

Protein association changes in the Hedgehog signaling complex mediate differential signaling strength

Cecile Giordano[1,*], Laurent Ruel[1,*,‡], Candice Poux[2] and Pascal Therond[1,‡]

ABSTRACT

Hedgehog (Hh) is a conserved morphogen that controls cell differentiation and tissue patterning in metazoans. In *Drosophila*, the Hh signal is transduced from the G protein-coupled receptor Smoothened (Smo) to the cytoplasmic Hh signaling complex (HSC). How activated Smo is translated into a graded activation of the downstream pathway is still not well understood. In this study, we show that the last amino acids of the cytoplasmic tail of Smo, in combination with G protein-coupled receptor kinase 2 (Gprk2), bind to the regulatory domain of Fused (Fu) and highly activate its kinase activity. We further show that this binding induces changes in the association of Fu protein with the HSC and increases the proximity of the Fu catalytic domain to its substrate, the Costal2 kinesin. We propose a new model in which, depending on the magnitude of Hh signaling, Smo and Gprk2 modulate protein association and conformational changes in the HSC, which are responsible for the differential activation of the pathway.

KEY WORDS: Signaling, *Drosophila*, Hedgehog, Smoothened, Gprk2, Fused, Differential phosphorylation, Protein association change

INTRODUCTION

The Hedgehog (Hh) family of secreted proteins is conserved through evolution and is involved in numerous biological processes during development and adult life, including tissue organization, cell proliferation and stem cell homeostasis in metazoans (Briscoe and Thérond, 2013). The Shh signaling pathway in humans has been implicated in the genesis of several types of cancer (Scales and de Sauvage, 2009) and genetic syndromes (Athar et al., 2014). Therefore, elucidating the mechanisms involved in Hh signal transduction is of interest to developmental biologists and also to oncologists.

The Hh receptor Patched (Ptc), is a transmembrane protein that constitutively represses Hh signaling (Hooper and Scott, 1989; Nakano et al., 1989). The binding of Hh to Ptc inhibits its repression of Smoothened (Smo), a member of the G protein-coupled receptor (GPCR) superfamily (Robbins et al., 2012). An important step in the activation of Smo relates to its conformational change; in the absence of Hh, inactive Smo is present as a dimer, in which the cytoplasmic tails are in a closed conformation, which leads to its degradation (Zhao et al., 2007; Li et al., 2012; Xia et al., 2012). This conformation is maintained by electrostatic interactions between positively and negatively charged clusters in the C–terminal domain. Hh activation neutralizes the positively charged cluster by triggering the phosphorylation of an adjacent domain (Zhao et al., 2007). In *Drosophila*, this phosphorylation is sequential and triggered by several kinases that include protein kinase A (PKA; PKA-C1 – FlyBase), the serine-threonine kinase Fused (Fu) and G protein-coupled receptor kinase 2 (Gprk2), which promote the conversion of Smo to an open conformation (Zhang et al., 2004; Jia et al., 2004; Apionishev et al., 2005; Zhou et al., 2006; Jia et al., 2010; Chen et al., 2010; Fan et al., 2012; Jiang et al., 2014; Maier et al., 2014; Li et al., 2016; Sanial et al., 2017). This switch seems to be essential for the cell surface accumulation of Smo and the activation of signaling. Differences in the strength of Hh signaling are generated by the gradual phosphorylation of Smo. Smo activation leads to the activation of Cubitus interruptus (Ci), the only known transcriptional mediator of the Hh response (Alexandre et al., 1996). Ci is a bifunctional transcription factor that can both activate (Ci-Act) or inhibit (Ci-Rep) transcription (Whitington et al., 2011; Méthot and Basler, 1999).

The cascade of events linking the activation Smo protein and Ci is still a matter of debate. In the absence of Hh, full-length Ci (Ci155) undergoes sequential phosphorylation at multiple sites, by different kinases including the priming kinase PKA, leading to a partial degradation of the C-terminal transactivation domain (Price and Kalderon, 2002; Jia et al., 2005; Smelkinson et al., 2007; Smelkinson and Kalderon, 2006; Tian et al., 2005) and the formation of Ci-Rep (Aza-Blanc et al., 1997; Méthot and Basler, 1999). The activation of Smo inhibits the partial proteolytic processing of Ci, allowing Ci155 to act as a transcriptional activator (Alexandre et al., 1996).

The master regulator of Ci activity is a protein complex composed of Fu (Préat et al., 1990) and the kinesin protein Costal2 (Cos2) associated with the Smo cytoplasmic tail (Sisson et al., 1997; Robbins et al., 1997; Jia et al., 2003; Ogden et al., 2003; Lum et al., 2003; Ruel et al., 2003; Aza-Blanc et al., 1997). The Hh signaling complex (HSC) directly controls the post-translational regulation and nuclear translocation of Ci (Robbins et al., 1997; Chen et al., 1999; Wang et al., 2000; Wang and Holmgren, 1999). Interestingly, the HSC is used as a scaffold that brings kinases with dual activity, such as PKA, in proximity to Ci and Smo (Zhang et al., 2005; Ranieri et al., 2014; Li et al., 2014). It has been proposed that Hh signaling increases the level of Smo, which binds to the HSC and outcompetes Ci for association with PKA, causing a switch in PKA substrate recognition from Ci to Smo (Ranieri et al., 2014).

The activation of the HSC involves its direct interaction with Smo (Ruel et al., 2003; Lum et al., 2003; Jia et al., 2003; Ogden et al., 2003). Fu consists of an N-terminal catalytic domain and a C-terminal regulatory domain (Fu-Reg). Fu-Reg interacts with several proteins of the HSC: Cos2 (Robbins et al., 1997; Sisson

[1]Université Côte d'Azur, CNRS, Inserm, iBV, 06108 Nice, France. [2]Stockholms Universitet, Wenner-Grens Institut, SE-106 91 Stockholm, Sweden.
*These authors contributed equally to this work

‡Authors for correspondence (therond@unice.fr; ruel@unice.fr)

P.T., 0000-0003-0434-2334

DEVELOPMENT

1

et al., 1997), Smo (Malpel et al., 2007; Sanial et al., 2017) and PKA (Ranieri et al., 2014). Moreover, it has been proposed that Fu-Reg interacts with the Fu catalytic domain, blocking the kinase activity in the absence of Hh. In contrast, this association would be inhibited upon Hh signaling, allowing Fu catalytic activation, autophosphorylation and possibly dimerization (Ascano and Robbins, 2004; Robbins et al., 1997; Zhou and Kalderon, 2011; Zhang et al., 2011; Shi et al., 2011).

Once activated, several post-translational changes are observed within the HSC, including the Fu-dependent phosphorylation of Cos2 on two residues, serine 572 (S572) and serine 931 (S931) (Nybakken et al., 2002). Cos2 phosphorylation can serve as *in situ* indicators of Hh signaling in tissues in which Hh is active (Raisin et al., 2010). In the wing imaginal disc, Hh is expressed in the posterior (P) compartment and activates different cellular targets, depending on their distance from the Hh source. *In vivo*, low-to-high magnitude Smo activation in the anterior (A) cells differentially activates downstream Fu kinase activity and the phosphorylation of Cos2, from single phosphorylation (S572P) at low levels to double phosphorylation (S572P-S931P) at higher levels of signaling (Ranieri et al., 2012). Moreover, Gprk2 is required for the Smo-dependent activation of target genes at high levels and, consequently, for the phosphorylation of S931, but not for that of S572 (Ranieri et al., 2012). Nevertheless, the mechanism by which the differential conformation of Smo is transduced into different levels of Fu kinase activation is not known.

Here, we present new data on the link between activated Smo and Fu catalytic activity, and, more specifically, on the differential levels of Fu kinase activation. We show that the binding of the terminal domain of the cytoplasmic tail (the last 52 amino acids) of Smo with Fu-Reg triggers Fu catalytic activation at a high level, thus acting as a Fu-activating peptide. In addition, we found that the Smo-Fu binding triggers a change within the Fu protein, which brings the Fu catalytic domain into closer proximity to its substrate, Cos2. We propose a new model in which, depending on the magnitude of Hh signaling, Smo induces a conformational change in Fu within the HSC, which is a crucial step for the transduction of the Hh extracellular gradient into differential gene responses.

RESULTS
Identification of a Smo peptide that behaves as a Fu activator

In order to better understand the mechanism by which the Smo protein activates the Hh pathway, we conducted an *in vivo* structure-function analysis of Smo to identify the domain(s) involved in downstream activation. At a low level of Hh signaling, the partial proteolysis of Ci is repressed, resulting in the expression of the Hh transcriptional target *decapentaplegic* (*dpp*; Méthot and Basler, 1999), whereas at high levels of signaling, Ci is converted to CiA, leading to the expression of the two targets, *ptc* and *engrailed* (*en*), in the first three rows of A cells at the A/P border (Fig. 1A,B). Three overlapping domains of the Smo cytoplasmic tail, Smo^{Cyto} [555-1036 amino acids (aa)], Smo$^{\Delta SAID}$ (818-1036 aa) and Smo^{Fu} (985-1036 aa) (Fig. 1C), were evaluated for their ability to activate expression of *hh* targets in the dorsal compartment of imaginal discs (Fig. 1D-I″). In all these *in vivo* assays, the ventral domain serves as an internal control because ventral cells are wild type.

Surprisingly, we found that, of the three Smo cytoplasmic constructs, the smallest domain of Smo (Smo^{Fu}, corresponding to the last 52 aa), is the most potent inducer of the pathway (Fig. 1H-I″). Indeed, the impact of Smo^{Fu} on high signaling activation is clearly visible in the case of the anterior enlargement of Ci-A, Ptc and En (Fig. 1H-I″). To confirm this result, Smo^{Fu} was constitutively expressed throughout the entire pouch of the imaginal disc

(Fig. S1A). Consequently, Ci-A, Ptc and En expression domains were expanded (Fig. S1A-A″) and the corresponding adult wings displayed an increase in the vein 3 and 4 interspace, which is characteristic of increased activation of Hh signaling (Fig. S1A‴).

To confirm the effect of the C-terminal domain of Smo, we used a truncated variant of Smo lacking 59 aa from the C-terminus (SmoΔFu; Fig. 1C; Malpel et al., 2007). Compared with Smo-WT and Smo^{Fu}, SmoΔFu induced a much weaker increase in Ptc upregulation (compare Fig. 1J and K), indicating that depletion of the last 59 aa of Smo impairs full Smo activation. Consistently, phosphorylation sites of the C-terminal domain of Smo (916-1036 aa), which overlap Smo^{Fu} residues, have been shown to promote Smo activation (Sanial et al., 2017). Finally, signaling activity of SmoΔFu was rescued upon co-expression with Smo^{Fu} (Fig. 1L, Fig. S1B) to a level equivalent to that of Smo-WT (Fig. 1J, Fig. S1C-E).

Because endogenous Smo and phospho-Smo pattern is not modified by the expression of Smo^{Fu} in the wing disc, we believe that Smo^{Fu} is not modifying endogenous Smo regulation (Fig. S2A-D). Alternatively, because the last 59 aa of Smo are able to co-immunoprecipitate with Fu and bind directly to Fu in a two-hybrid screen (Fig. S2E; Malpel et al., 2007), we decided to test the ability of Smo^{Fu} to activate the Fu kinase both *in vitro* and *in vivo*. We have previously demonstrated that Cos2 phosphorylation at S572 and S931 can serve as indicators of differential Fu activation (Fig. 2A,B). It is known that Cos2 phosphorylation is abrogated in the absence of Hh signaling; for example, in cells expressing the dominant-negative form of Smo, Smo-AAA (Fig. 2C, Fig. S2F), compared with those expressing the wild-type (WT) form, Smo-WT (Fig. 2D, Fig. S2F). Similar to our previous observation in the wing discs, we found that Smo^{Fu} is the most potent inducer of Cos2 phosphorylation compared with the other Smo cytoplasmic constructs when expressed in *Drosophila melanogaster* Schneider 2R+ (S2R+) cells (Fig. S2F). *In vivo*, expression of Smo^{Fu} leads to an increase in Cos2 phosphorylation, which was mostly visible on S931 (Fig. 2E-F′). In this context, the endogenous expression pattern of Cos2 was not modified with respect to the ventral control (Fig. S2A). Given that Cos2 phosphorylation of S572 and S931 depends on Fu activity (Fig. S3A; Ranieri et al., 2012), this suggests that the last 52 aa of Smo are sufficient to act as a Fu kinase-activating peptide. Interestingly, both *in vivo* and *in vitro*, SmoΔFu, which displays a weaker interaction with Fu (Fig. S3B), is unable to activate cellular targets or Fu to a high level, in terms of S931 phosphorylation, but is still able to induce phosphorylation of Ser572 (Fig. 2G-H′, Fig. S3A-C″). To confirm this hypothesis, endogenous Smo in the dorsal compartment was depleted by RNA interference (RNAi), and the activity of SmoΔFu was tested in this new background. The double-strand RNA (dsRNA) sequence targeted against *smo* is located at the 5′ end of the *smo* transcript (Sanial et al., 2017), a sequence which is not present in the SmoΔFu transgene. The *smo* RNAi-dependent defects were shown to be fully rescued by a Smo-WT transgene (Sanial et al., 2017; Maier et al., 2014). The expression of SmoΔFu in cells depleted for Smo by RNAi revealed that phosphorylation of S931 and expression of En/Ptc cannot be sustained by SmoΔFu (Fig. 2J′,K′, L, Fig. S3D). Finally, signaling activity of SmoΔFu rescued the Ser931 pattern upon co-expression with Smo^{Fu} (Fig. 2I, quantification in Fig. S3E). Note that the pattern of endogenous Cos2 is not modified with respect to the ventral control by Smo^{Fu} or SmoΔFu (Figs S2A and 3C). From this, we conclude that the last 52 aa of Smo are able to interact with Fu, which stimulates its kinase activity and promotes signal transduction at the highest level.
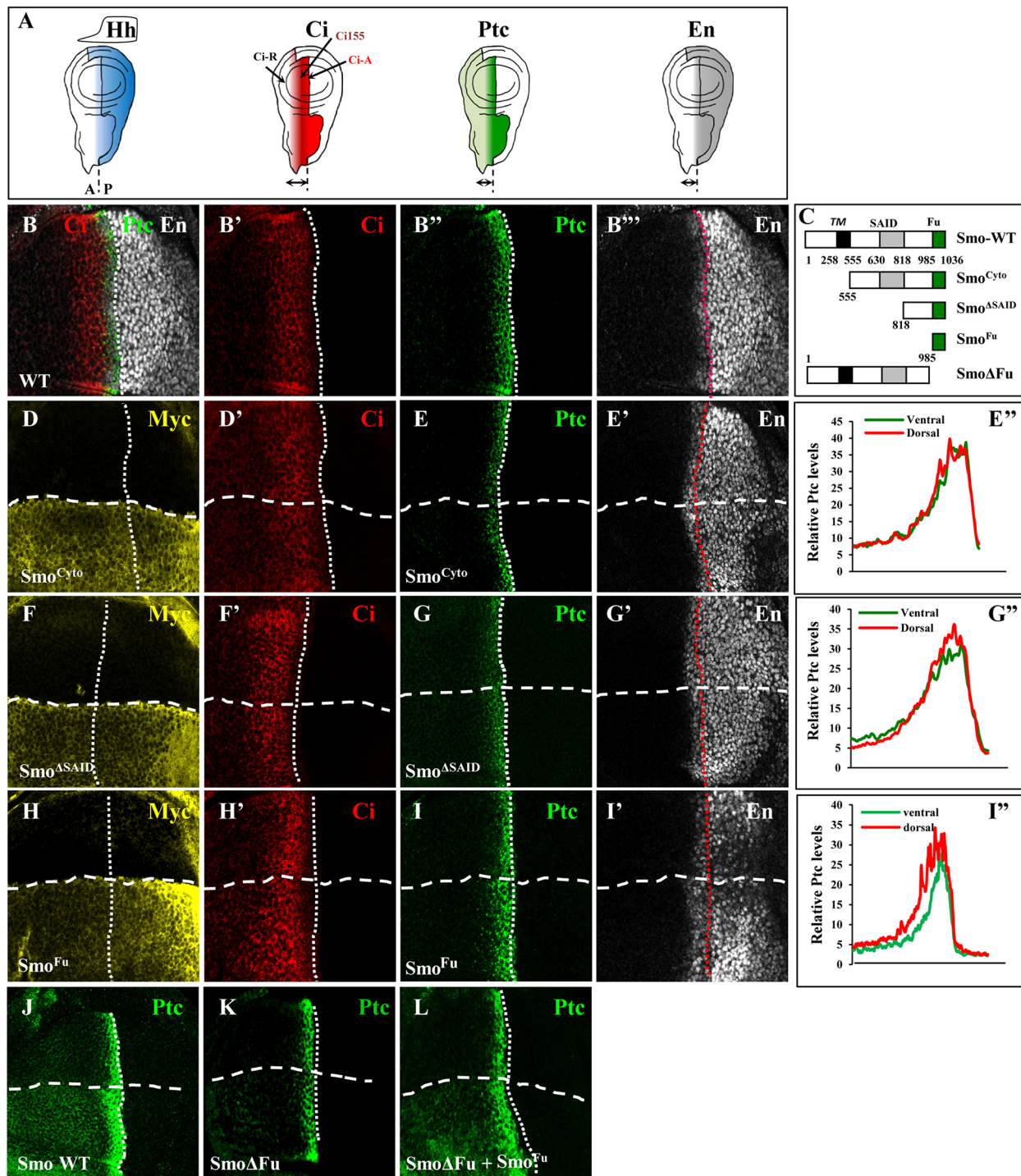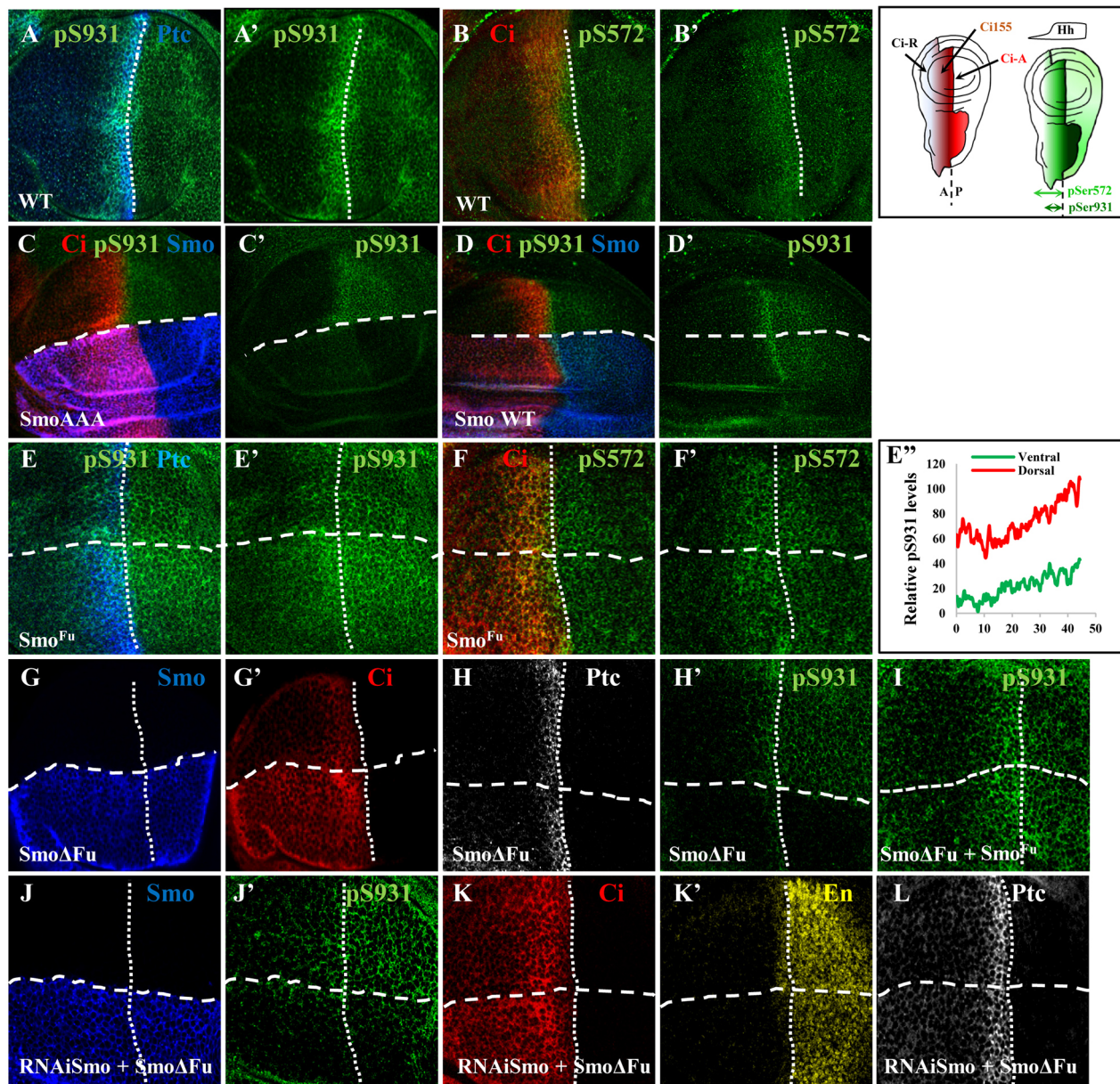
Fig. 1. The last 59 amino acids of Smo activate the Hh pathway. (A) Schematic distribution of Hh, Ci isoforms, En and Ptc in the wing imaginal disc. The double heads represent the domain induced by Hh in the anterior compartment. (B) Wild-type wing discs stained for Ci155 (red, B,B′), Ptc (green, B,B″) and En (gray, B,B‴). (C) Scheme of the Smo-WT protein and the Smo variants. (D-I″) Wing discs expressing Smo^{Cyto}-Myc (D-E′), Smo ^{ΔSAID}-Myc (F-G′) or Smo^{Fu}-Myc (H-I′) driven by *apterous*-Gal4 (*ap*-Gal4) were immunostained for Myc (yellow, D,F,H), Ci155 (red, D′,F′,H′), Ptc (green, E,G,I) and En (gray, E′,G′,I′). Related quantification graphs (*n*=5 discs) of Ptc (E″,G″,I″) staining in the anterior compartment are shown on the right. (J-L) Wing discs expressing Smo-WT (J), SmoΔFu (K) or SmoΔFu and Smo^{Fu} (L) driven by *ap*-Gal4 and stained for Ptc (green, J,K,L). Note that the co-expression of Smo^{Fu} with SmoΔFu gives the same phenotype as the expression of Smo-WT. For all images, wing discs are shown ventral uppermost with the posterior on the right, and the anterior (A)/posterior (P) border is indicated by dotted lines and the dorsal/ventral border by dashed lines.

The potency of the Fu-activating peptide depends on endogenous Smo and Gprk2

During this study we noticed that Smo^{Fu} did not induce signaling distal to the A/P border in the most anterior cells (Fig. 1H′,I). To know whether the activity of Smo^{Fu} depends on the presence of endogenous Smo, the activity of Smo^{Fu} was tested in cells depleted for endogenous Smo expression (Fig. 3A). In this background, Ptc expression was inhibited (Fig. 3B‴) and Ci155 was not stabilized

Fig. 2. The last 59 amino acids of Smo promote Fu kinase activity. The scheme in the top right-hand corner represents the distribution of Ci isoforms and pSer572/pSer931 Cos2. (A-B′) Wild-type wing discs stained for Cos2-pS931 (green, A,A′), Cos2-pS572 (green, B,B′), Ptc (blue, A) and Ci155 (red, B). (C-H′) Wing discs expressing inactive Smo-AAA (C), Smo-WT (D), Smo^{Fu}-Myc (E-F′) or SmoΔFu (G-H′) in the dorsal compartment were immunostained for Ci155 (red, C,D,F,G′), pS931 (green, C,C′,D,D′,E,E′,H′), pS572 (green, F,F′), Smo (blue, C,D,G) and Ptc (blue, E and gray, H). (E″) Quantification of Fu activity by following the levels of Cos2 phosphorylation on serine 931 in wing discs expressing Smo^{Fu} (E) (n=4 discs). (I) Wing discs expressing SmoΔFu with Smo^{Fu} driven by *ap*-Gal4 and stained for pS931 (green, I). Note that the co-expression of SmoΔFu with Smo^{Fu} gives the same phenotype as the expression of Smo-WT (D). (J-L) Wing discs expressing dsRNA against endogenous Smo with SmoΔFu expressed in the dorsal compartment were immunostained for Smo (blue, J), pS931 (green, J′), Ci155 (red, K), En (yellow, K′) and Ptc (gray, L).

(Fig. 3B″), suggesting that Smo^{Fu} was no longer able to activate the Hh pathway.

From this, we hypothesized that the presence of full-length Smo enhances the ability of the Smo^{Fu} peptide to trigger Fu activity. We thus investigated whether the association of Smo^{Fu} with Fu was modified by the presence of activated full-length Smo. Interestingly, we found that, in the absence of Smo and Hh, Smo^{Fu} associates poorly with Fu, but this association is greatly increased in the presence of Smo and Hh (Fig. 3G, compare lanes 2 and 6, with similar amount of Smo^{Fu}). This indicates that, at high levels of signaling, the accessibility and interaction of the Smo^{Fu} peptide with

the regulatory domain of the Fu is increased. This suggests that although the Smo^{Fu} peptide is sufficient to interact with Fu, the rest of Smo plays a role, possibly changing the Fu protein conformation, enhancing this interaction.

To confirm this, we analyzed the activity of Smo^{Fu} in a background depleted for *gprk2* in which Hh signaling is less likely because Smo is not converted to a fully open conformation (Chen et al., 2010; Molnar et al., 2007). In the *gprk2* mutant, the Hh signal was reduced to a lower level at the A/P border, with the loss of expression of anterior *en* (Fig. 3C′, Fig. S4A′) and *ptc* (Fig. 3D′, Fig. S4B′), and with an extension of Smo
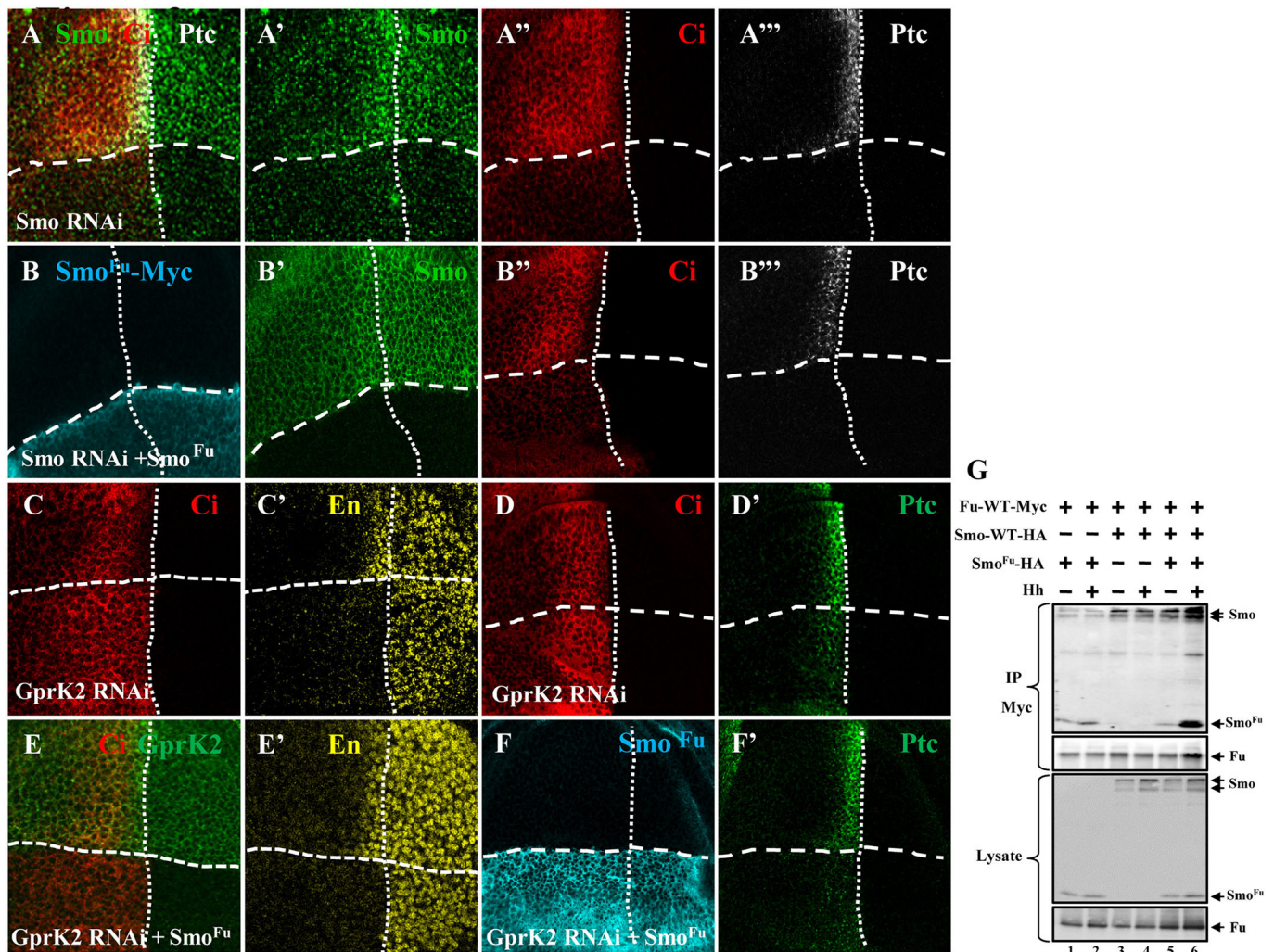
Fig. 3. The effect of the last 59 amino acids of Smo requires the presence of endogenous Smo. (A-B‴) Wing discs expressing dsRNA against Smo without (A) or with (B) Smo^Fu-Myc by using an *ap*-Gal4 driver and immunostained for Ci155 (red, A,A″,B″), Ptc (gray, A,A‴,B‴), Smo (green, A,A′,B′) and Myc (blue, B). (C-F′) Wing discs expressing dsRNA against Gprk2 without (C-D′) or with (E-F′) Smo^Fu-Myc driven by *ap*-Gal4 were stained for Ci155 (red, C,D,E), En (yellow, C′, E′), Ptc (green, D′,F′), Gprk2 (green, E) and Myc (blue, F). (G) S2R+ cells were transfected with the indicated constructs. The lysates were immunoprecipitated for Fu-WT-Myc using an anti-Myc antibody, and analyzed for the presence of Smo-WT and Smo^Fu using an anti-HA antibody.

phosphorylation and stabilization (Fig. S4C′,C″). We also observed a limited Fu kinase activity, which allowed the phosphorylation of Cos2 on serine 572 (Fig. S4A), but not on serine 931 (Fig. S4B). The analysis of Fu electrophoretic shift observed upon Hh signaling activation (a mark of Fu autophosphorylation) in the presence of different variants of Gprk2 did not show any evidence of direct phosphorylation of Fu by Gprk2 (Fig. S4F). Interestingly, we found that, in the absence of *gprk2*, Smo^Fu was not able to activate Hh signaling (Fig. 3E-F′) and phosphorylation of Cos2 on serine 931 (Fig. 4A). The *gprk2* phenotype could be rescued by reintroducing the expression of a wild-type form of Gprk2 (Fig. 4B,B′), but not by the kinase-dead version of Gprk2, Gprk2-KD (Fig. 4C,C′, Fig. S4D-D″). In the rescued animal (Fig. 4D), Smo^Fu is able to promote high Hh signaling (compare Fig. 4E,E′ with Fig. S4E-E″, and see quantification in Fig. 4D″,E″). To confirm the requirement of Gprk2-modified Smo to fully activate Fu, we compared the activity of two variants of Smo, SmoSD123 (Fig. 4F-G), mimicking a PKA phosphorylated variant, and Smo-GPSA (Fig. 4H-I), in which Gprk2 sites at S741/S742 and S1013/

S1015 positions have been replaced by alanine in SmoSD123 (Chen et al., 2010). We could show that the Smo-GPSA variant is unable to promote phospho-S931 (Fig. 4I), but does induce S572P (Fig. 4H′).

These results reveal that the effect of the Fu-activating peptide not only requires the presence of Smo, but requires a Smo protein which is activated by the kinase activity of Gprk2.

Association of Smo with the Fu kinase
In order to analyze the association of Smo with Fu, we used the multicolor bimolecular fluorescence complementation (BiFC) technique in S2R+ cells (Shyu and Hu, 2008). Two nonfluorescent fragments of a cleaved fluorescent protein (YFP) were separately fused to the Smo and Fu proteins. Fusion of the two YFP moieties was designed at the C-terminal (C-term) end of the wild-type Smo (Ranieri et al., 2014) and at the N-terminal (N-term) of the wild-type Fu protein, and does not affect Smo and Fu activities (data not shown). Additional epitope sequences [Myc or hemagglutinin (HA)] were also inserted in order to localize these proteins in the cells by immunofluorescence (Fig. 5). This technique enables quantification

DEVELOPMENT

5
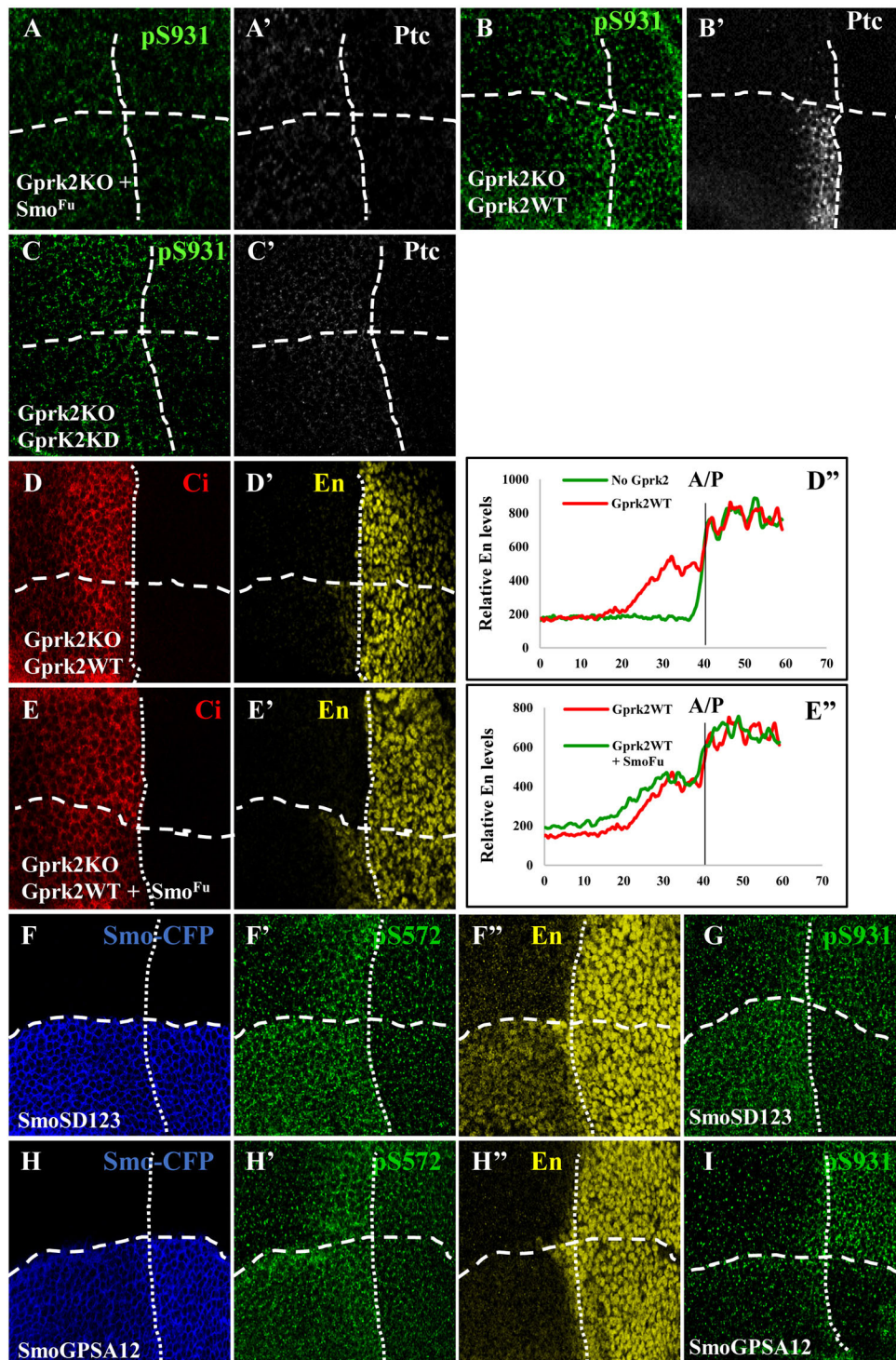
Fig. 4. The effect of the last 59 amino acids of Smo requires the presence of Gprk2 activity. (A-C) Wing discs from *gprk2* knockout (KO) mutant discs expressing either Smo[Fu] (A), Gprk2-WT (B) or Gprk2-KD (C) in the dorsal compartment were stained for pS931 (green, A,B,C) and Ptc (gray, A′,B′,C′). (D,D′,E,E′) *gprk2* KO mutant discs expressing Gprk2-WT alone (D) or with Smo[Fu]-Myc (E) under *ap*-Gal4 driver were stained for Ci155 (red, D,E) and En (yellow, D′,E′). (D″) Quantification of En intensity in *gprk2* KO mutant discs (green) in which Gprk2-WT has been expressed in the dorsal compartment (red) (*n*=4 discs). (E″) Quantification of En intensity in *gprk2* KO mutant discs expressing Gprk2-WT (red) or Gprk2-WT and Smo[Fu] (green) (*n*=4 discs). (F-I) Wing discs expressing SmoSD123-CFP (F-G) and SmoGPSA12-CFP (H-I) driven by *ap*-Gal4 were stained for Smo-CFP (blue, F,H), pS572 (green, F′,H′), En (yellow, F″,H″) and pS931 (green, G,I).

of the interaction between Smo-N-YFP and C-YFP-Fu in the cells, which brings the two nonfluorescent fragments into close proximity, thereby reconstituting an intact fluorescent YFP (Fig. 5A-F‴). After transfection and differential treatment with Hh, we found a significant increase in Smo-Fu association upon treatment with Hh, which was further enhanced upon co-transfection with PKA and Gprk2 (Fig. 5C-F‴, and quantification in G). Also, this treatment led to a strong accumulation of the YFP signal at the plasma membrane, where Smo is stabilized (Fig. 5F). As control, expression of either Smo-N-YFP (Ranieri et al., 2014) or C-YFP-Fu alone did not

induce YFP reconstitution at a significant level (Fig. 5A-B‴, and quantification in H).

Our data strongly suggest that Hh signaling promotes Smo and Fu association. It is important to note that in this set up, *ptc* expression is very low and is not modulated by the Hh pathway, as these cells do not express Ci, the transcriptional regulator of *ptc* expression. To conform more to the *in vivo* situation in which Ptc level is highly increased in Hh-receiving cells, we analyzed the BiFC signal from Smo-N-YFP association with C-YFP-Fu in cultured S2R+ cells in which we had increased the level of Ptc
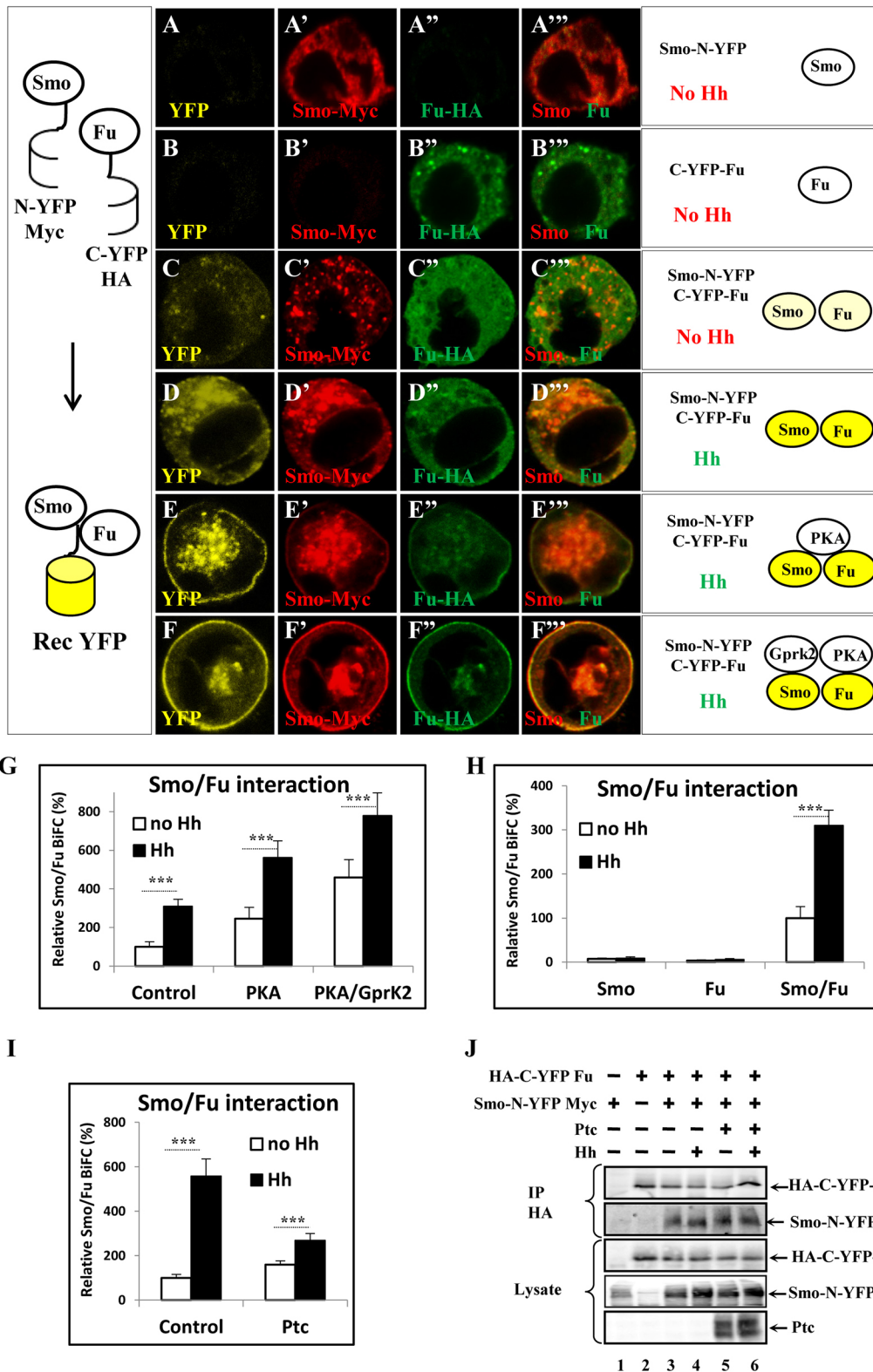
Fig. 5. See next page for legend.

(Fig. 5I). In these cells, the BiFC signal was significantly reduced. Note that the amount of Smo-N-YFP immunoprecipitated with C-YFP-Fu-WT in either the absence or presence of Ptc (Fig. 5J, compare lanes 4 and 6) was not significantly different, suggesting that the full association of Smo with Fu was not decreased in the presence of Ptc, but raising the possibility that Ptc mediates the decrease in the association of the Smo-C-term with Fu-N-term domain within the Smo/Fu complex.

Fig. 5. The association of Smo with Fu is enhanced in the presence of Hh.
(A-F‴) S2R+ cells with or without Hh treatment were transfected with Smo-N-YFP-Myc (A-A‴,C-F‴) and HA-C-YFP-Fu-WT (B-F‴) individually or together. Scheme of YFP reconstituted activity is represented on the left, while the experimental conditions and structure of the protein complex are indicated on the right of each row of images. Transfected cells were stained for Myc (red, A′,B′,C′,D′,E′,F′,A″,B‴,C‴,D‴,E‴,F‴) and HA (green, A″,B″,C″,D″,E″, F″,A‴,B‴,C‴,D‴,E‴,F‴). YFP signals were detected in yellow (A,B,C,D,E,F). (G) Quantification of YFP reconstitutions between Smo and Fu interactions in the conditions shown in Fig. 5C-F‴. Note that adding PKA or PKA+Gprk2 increase the baseline, likely due to their effect on Smo conformation. (H) Quantification of the YFP signal in the transfection conditions shown in A-D‴. Individually, no YFP signals are detected in A and B conditions in the absence or presence of Hh. For all BiFC quantification, YFP signals were analyzed in 150-200 cells. Data are the means±s.d from three biological replicates; ***$P<0001$. (I) Quantification of Smo/Fu BiFC in S2R+ cells treated with Hh and overexpressing Ptc (means±s.d. from three biological replicates; ***$P<0001$). (J) Constructs expressing HA-C-YFP-Fu-WT, Smo-WT-N-YFP-Myc and Ptc were transfected in S2R+ cells treated with or without Hh. Cell lysates were immunoprecipitated with an antibody against HA, and Smo was detected with an antibody against Myc. The comparison between lanes 4 and 6 shows a similar level of Smo associated with Fu.

In vivo reconstitution of the Smo-Fu interaction

To confirm the interaction of Smo with Fu *in vivo*, we conducted BiFC in wing discs. Both C-YFP-Fu-WT and Smo-N-YFP constructs were expressed uniformly throughout the dorsal compartment (Fig. S5A). Expression of either Smo-N-YFP or C-YFP-Fu-WT alone did not induce YFP reconstitution at a significant level (Ranieri et al., 2014; Fig. S5B-C″). As expected, the co-expression of Smo-N-YFP and C-YFP-Fu-WT in P cells revealed a constant BiFC signal confirming the close Smo-C-term/Fu-N-term association in Hh-activated cells (Fig. 6A,A‴). Interestingly, expression of the two constructs in the anterior compartment revealed a strong modulation of the BiFC signal. In the first row of A cells, the BiFC signal between Smo and Fu was very low, suggesting a decrease or change in the association between the proteins in A cells. This domain correlates with high Hh signaling level, with elevated level of Ptc (Fig. 6A) and Cos2 phosphorylation on S931 (Fig. S5D′). We also observed that in more anterior A cells, the BiFC signal initially increased but ultimately decreased gradually in more distal A cells (Fig. 6A″,A‴). A similar BiFC profile was observed with a C-YFP-Fu-EE construct expressing a constitutive active Fu variant (Fig. 6B″), but was strongly modified upon expression of a kinase dead variant of Fu, C-YFP-Fu-KD (Fig. 6C″). The activities of these Fu variants were controlled, and showed that expression of either C-YFP-Fu-EE or C-YFP-Fu-KD modified the phosphorylation of Cos2, according to their expected activities (Fig. S5E-F″).

These data revealed a complex pattern of Smo association with Fu, which is regulated by differential levels of Hh signaling. To confirm that the decrease in the Smo-C-term/Fu-N-term association is due to the increase in Ptc levels in A cells, we analyzed the consequences of expressing dsRNA against *ptc* (Fig. 6D) or its transcriptional regulator *ci* (Fig. 6E). In both cases, this leads to the strong decrease of Ptc protein level, and thus should change the ratio between the receptor Ptc and its ligand Hh. We also analyzed *gprk2* mutant discs (Fig. 6F), which are characterized by the loss of Ptc upregulation at the A/P border (Fig. S4B′). In all three of these combinations, the decrease in the BiFC signal that we previously identified at the A/P border was no longer observed (Fig. 6D″,E″,F″).

Taken together, these data suggest that the modulation of the BiFC signal between Smo and Fu depends on the level of Hh signaling, and unexpectedly reveals a difference between P and A cells at the A/P border, both of which have high Hh signaling level.

Hh induces changes in Fu association with Cos2

To further understand how Smo association with Fu modifies downstream signaling, we chose to analyze how Smo binding to Fu modulates Fu activity and association with its substrate, Cos2. It has been previously shown that the last 57 aa of Fu-Reg bind to Cos2 protein, and that the overall association of Fu with Cos2 is not modulated by Hh signaling (Robbins et al., 1997; Ruel et al., 2007). Intriguingly, although Fu is constitutively associated with Cos2 (Robbins et al., 1997), it does not phosphorylate it to a significant level in the absence of Hh pathway activation. Thus, upon signaling activation, a modification of Fu which is already associated with Cos2 is necessary for Fu activation. Because Hh triggers Fu-dependent Cos2 phosphorylation within the protein complex *in vivo* (Ranieri et al., 2012), this suggests that a transient association between the catalytic domain of Fu and its target is modulated by Hh signaling and should be observable. We chose to separate the Fu protein into two parts, one corresponding to the Fu-Cat domain (from residues 1 to 302) encompassing all conserved residues present in the catalytic domain of the kinase protein family. The second part included the Fu-Reg domain (from residues 303 to 805), and corresponded to a protein region in which different components of the HSC associate directly (Fig. 7A; Aikin et al., 2008). The expression of the separated domains of Fu in cultured cells revealed that Fu-Reg associates with Fu-Cat (Fig. 7B). Interestingly, Fu-Cat displays only weak interaction with its substrate Cos2 (data not shown), and Cos2 phosphorylation is observed mainly in the presence of Fu-Reg, which conforms to previous data showing that the association of Fu with Cos2 involves the carboxyl terminus of Fu-Reg (Fig. 7C, compare lanes 1 and 2 with lanes 5 and 6; Robbins et al., 1997). We found that Fu-Reg residues from aa 303 to 422 (present in P1 and P6) and from 422 to 586 (present in P1 and P2) associate with Fu-Cat (Fig. S6B,C) and promotes Fu-Cat-dependent Cos2 phosphorylation (Fig. 7D). Together, these data suggest that association of Fu-Cat with Fu-Reg is necessary for Fu-Cat-dependent phosphorylation of Cos2.

In 2004, Ascano and Robbins proposed that, in the absence of Hh, an intracellular association of both Fu N-term and C-term domains inhibits Fu-Cat activity, whereas, upon Hh activation, the two domains dissociate, releasing the inhibition on the catalytic site (Ascano and Robbins, 2004). We thus tested the hypothesis that the binding of Smo to Fu-Reg could release Fu autoinhibition by inducing a dissociation of Fu-Reg from Fu-Cat. To test this hypothesis, we first performed co-immunoprecipitation of Fu-Reg and Smo[Cyto], and found that Smo did indeed bind Fu-Reg (Fig. 7E). Nevertheless, immunoprecipitation of Fu-Reg with Fu-Cat in the presence of Smo (Fig. 7E), or in the presence of an increasing amount of Smo (Fig. S6D), did not show a decrease in the association of Fu-Reg with Fu-Cat. From this, and contrary to what has been previously proposed, we concluded that the intramolecular association of Fu is likely not modulated by Smo.

To further analyze the mechanism of Fu activation by Hh signaling, we decided to focus on the regulation of Fu binding to its substrate Cos2 within the Cos2/Fu/Smo complex. To follow the possible changes of Fu already bound to Cos2, we hypothesized that Fu-Cat association with Cos2 could be modulated in the protein complex. For this, we analyzed the behavior of two constructs with YFP moieties, one fused to the N-term end of Fu-Cat and the other to the C-term end of Cos2 (scheme in Fig. 8A). After transfection, the BiFC analysis revealed a significant increase in the YFP signal between N-YFP-Fu-Cat and Cos2-C-YFP upon treatment with Hh, suggesting that signal activation leads to a change in the Fu-Cos2 complex which brings the two YFP moieties closer (Fig. S7A-F‴,
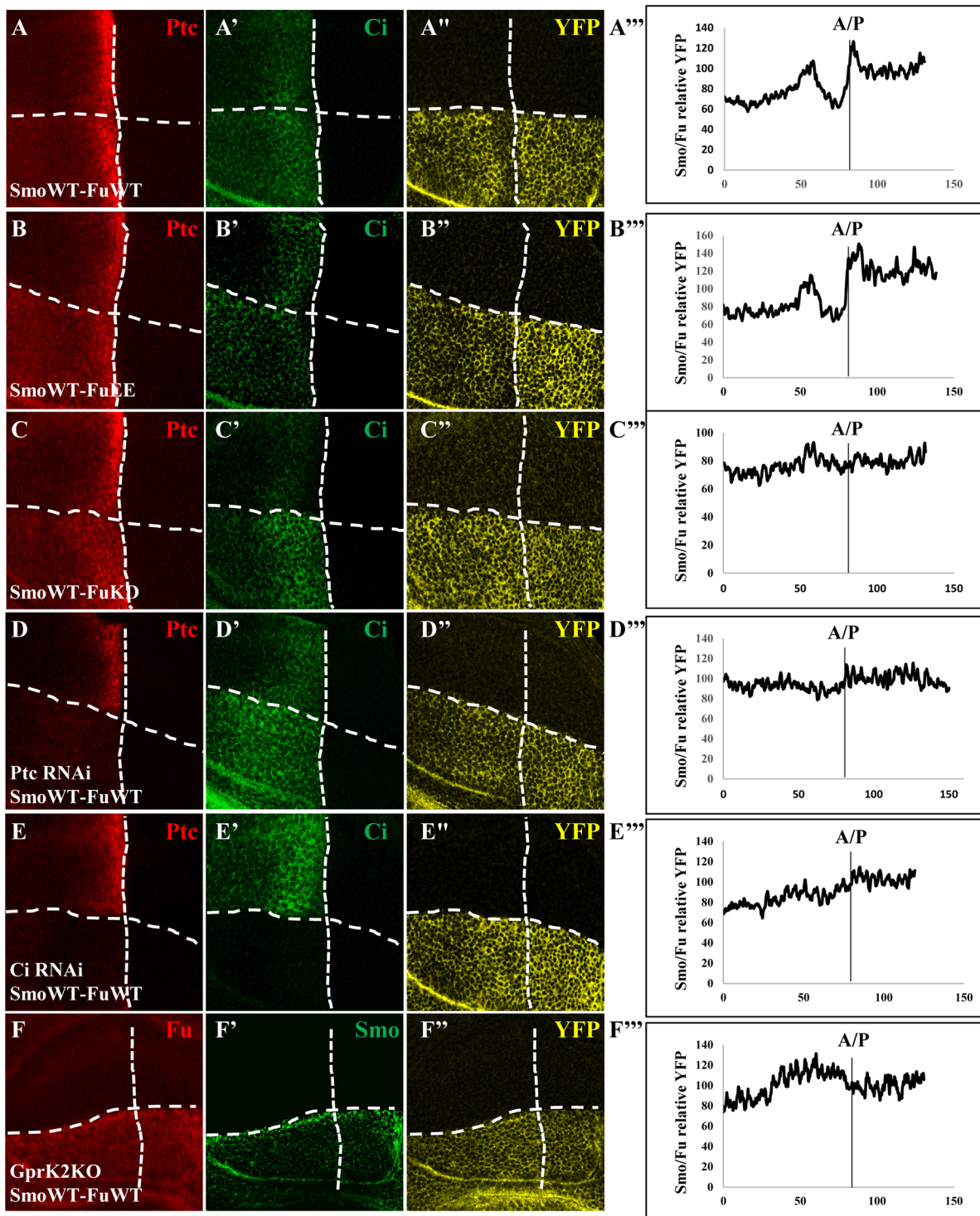
Fig. 6. Hh signaling modifies Smo association with Fu. (A-C‴) Wing imaginal discs co-expressing Smo-WT-N-YFP-Myc and HA-C-YFP-Fu-WT (A) or HA-C-YFP-Fu-EE (B) or HA-C-YFP-Fu-KD (C) in the dorsal compartment using the *ap*-Gal4 driver were stained for Ptc (red, A,B,C) and Ci155 (green, A′,B′,C′). YFP signals were detected in yellow (A″,B″,C″) and quantified (A‴,B‴,C‴) (*n*=5 discs). (D-F‴) Smo-WT-N-YFP-Myc and HA-C-YFP-Fu-WT are co-expressed in wing discs driven by *ap*-Gal4 with dsRNA against *ptc* (D) or *ci* (E) or in wing discs from *gprk2* KO mutant (F). Proteins were visualized in red (Ptc, D,E), green (Ci, D′,E′), red (Fu, F) and green (Smo, F′). YFP signals were detected in yellow (D″,E″,F″) and measured (D‴,E‴,F‴) (*n*=4 discs).

quantification in Fig. 8A). We also found an incremental change in the BiFC signal with these two constructs in the presence of a functional Gprk2. We confirmed that, under these conditions, the HSC complex is reconstituted, with the different members present in a stoichiometric manner (Fig. 8B), and that Cos2 is phosphorylated on S572 and S931 (Fig. 8A′). In this assay, levels of Cos2-C-YFP, N-YFP-Fu-Cat and Fu-Reg do not vary, suggesting that the increase in BiFC signal is not caused by an increase in protein stability
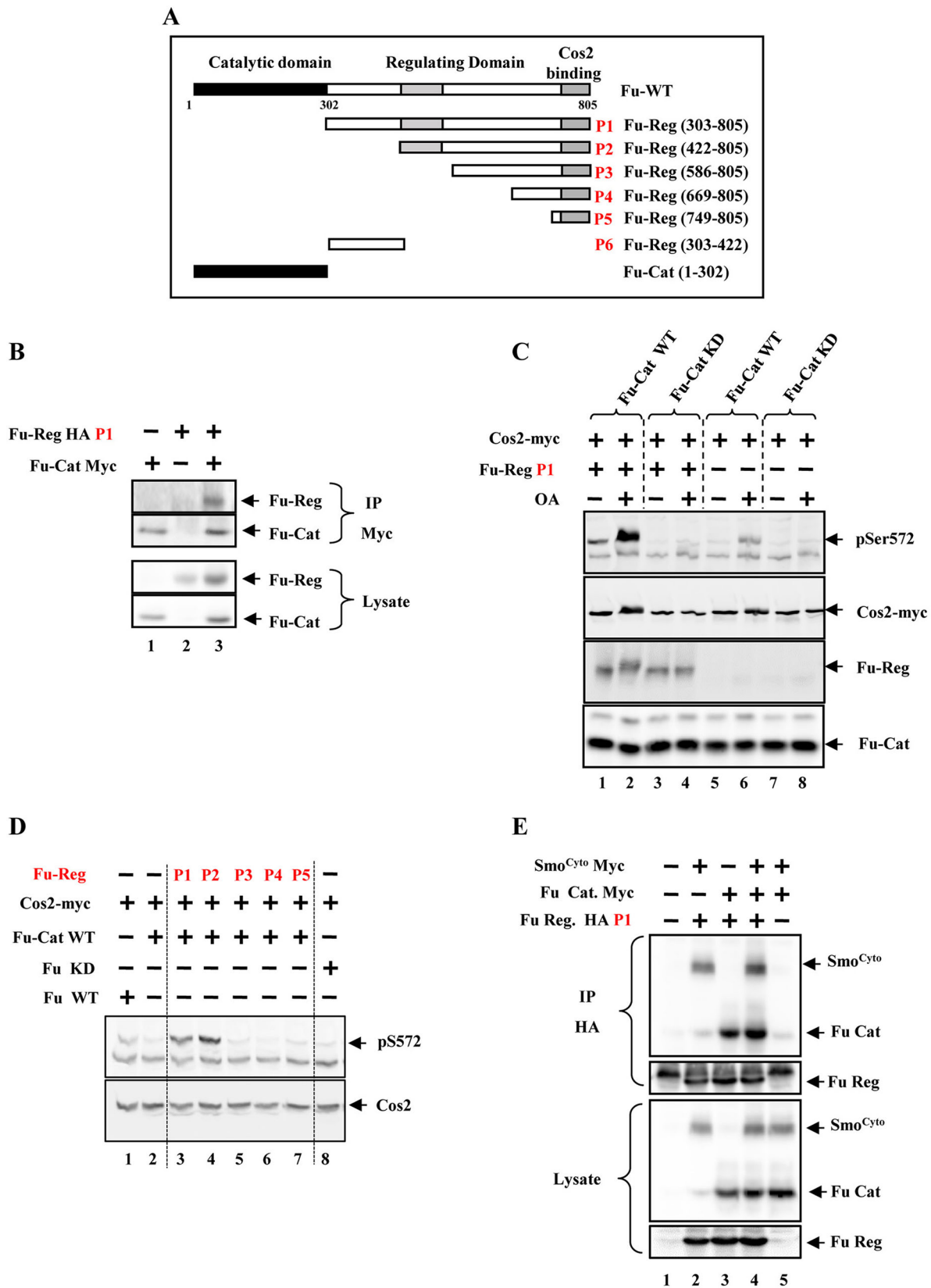
Fig. 7. Association of the Fu catalytic domain with the regulatory domain. (A) Scheme of Fu-WT and Fu variants with various deletions of its regulatory domain. Fu-Cat contains all aa present in the catalytic domain, whereas P1 contains all aa present in the Fu-Reg domain. P2 to P6 correspond to a truncated Fu-Reg domain. (B) S2R+ cells were transfected with the indicated constructs. Fu-Cat immunoprecipitates were analyzed for the presence of Fu-Reg. (C) Extracts of S2R+ treated with okadaic acid (OA) and transfected with the indicated constructs were analyzed by western blotting for the phosphorylation of Cos2. (D) Cells were transfected with the indicated constructs, and cell extracts were analyzed for Cos2 phosphorylation. (E) After transfection with the indicated constructs, Fu-Reg P1 immunoprecipitations were analyzed for the presence of Fu-Cat and Smo^Cyto. Note that Fu-Reg is not changing the level of Fu-Cat.
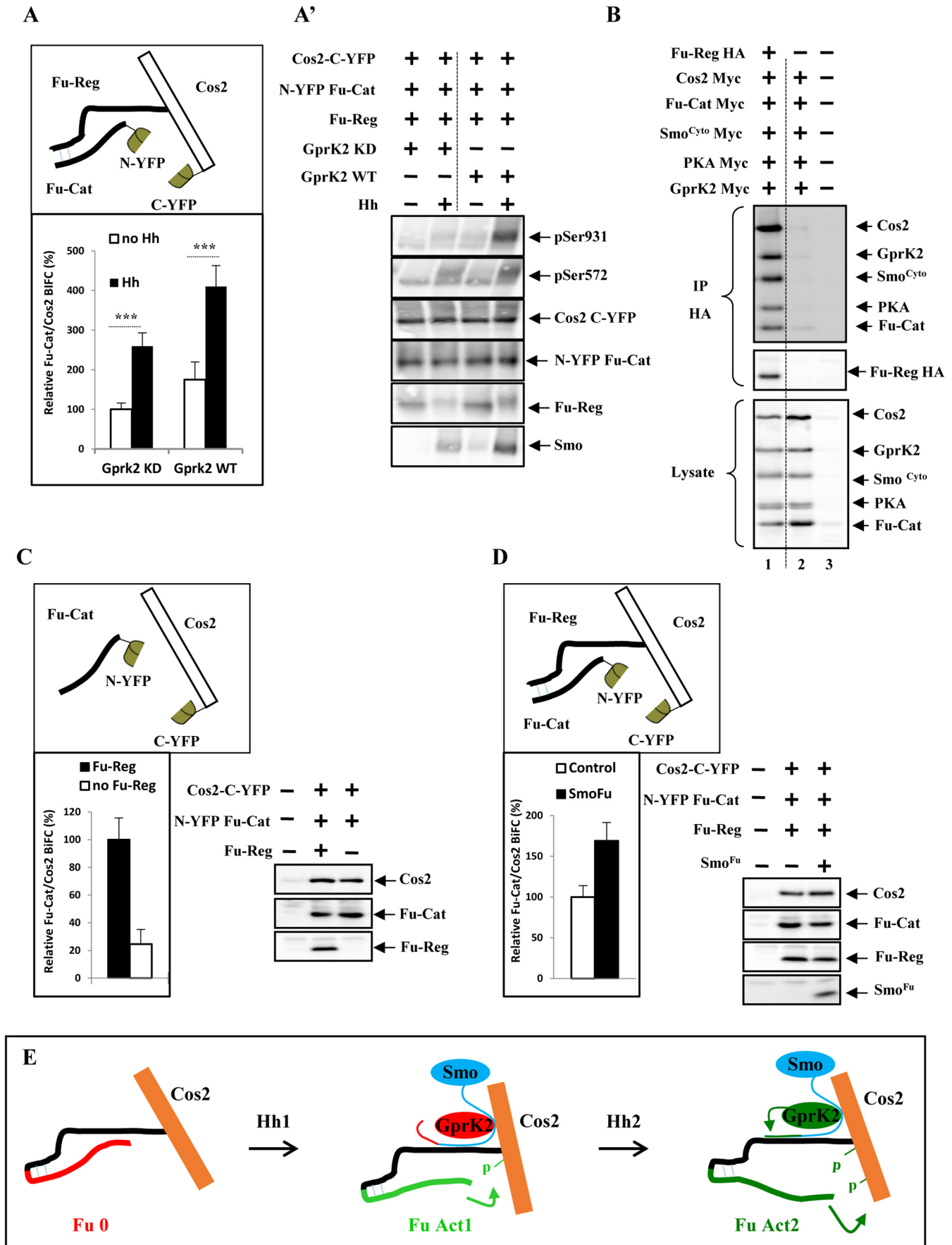
Fig. 8. See next page for legend.

Fig. 8. Change in Fu conformation induces differential Cos2 phosphorylation. (A-D) Schematic representation of Fu and Cos2 constructs used for the BiFC experiments. (A) S2R+ cells were transfected with N-YFP-Fu-Cat and Cos2-C-YFP in the presence of Fu-Reg and active (WT) or inactive (KD) Gprk2 variants. To reconstitute the HSC complex, PKA and Smo were also transfected with Hh. The graph represents the BiFC analysis between the Fu-Cat and Cos2 in different transfection conditions as indicated (means±s.d. of 100 cells from three biological replicates; ***P<0001). In A′, western blot analysis of lysates from cells described in A is representative of triplicate experiments. Note that the levels of Fu and Cos2 are not significantly changing in the presence of Hh. (B) Cells were transfected with different members of HSC tagged with a Myc sequence in the presence of Fu-Reg-HA as indicated, and Fu-Reg immunoprecipitates were analyzed for the presence of Myc-tagged proteins. Note that Fu-Reg forms a stoichiometric complex with HSC. (C) S2R+ cells were transfected with N-YFP-Fu-Cat and Cos2-C-YFP with or without Fu-Reg as shown on the western blot. The graph represents the BiFC analysis between the Fu-Cat and Cos2 constructs, depending on the presence or absence of Fu-Reg (means±s.d. of 100 cells from two biological replicates). (D) S2R+ cells transfected with the N-YFP-Fu-Cat, Cos2-C-YFP and Fu-Reg constructs, in the presence or absence of Smo^{Fu}. Cells were also transfected with Hh, Smo-WT, PKA and Gprk2. The western blot shows the levels of transfected proteins, and the graph represents the BiFC analysis between the Fu-Cat and Cos2 constructs (means±s.d. of 100 cells from two biological replicates). (E) Scheme recapitulating the Fu conformation changes in the Fu/Cos2 complex. In the absence of Hh, Fu is inactive. In the presence of Hh, stabilized Smo associates with the regulatory domain of Fu. Consequently, a Fu conformational change increases the proximity of the Fu catalytic domain with Cos2 and promotes Cos2 phosphorylation on Ser572. This leads to the first level of Fu activation (FuAct1). At high levels of signaling, the conformational changes of Smo C-terminal domains are reinforced by Gprk2-dependent phosphorylation and lead to a direct interaction of the C-terminal end of Smo with the Fu regulatory domain. This interaction enhances Fu activity and its proximity to Cos2, leading to the second level of Fu activation (FuAct2), promoting phosphorylation of Ser931.

(Fig. 8A′). We controlled the specificity of the BiFC increase by co-expressing the two YFP constructs without the Fu-Reg domain, which led to a significant decrease in the BiFC signal between Fu-Cat and Cos2 (Fig. 8C). These data suggest that activation of Hh signaling through Smo activation triggers a change in the Fu protein, which increases the proximity of Fu-Cat and its substrate Cos2, in order to promote full phosphorylation of Cos2. Interestingly, the expression of Smo^{Fu} in this set up also reinforces the proximity between N-YFP-Fu-Cat and Cos2-C-YFP in reconstituted protein complex, suggesting that the Fu-activating peptide is able to modify conformation of Fu in this assay (Fig. 8D).

DISCUSSION
Here, we present new data concerning the differential activation of the Fu kinase induced by Smo and the Gprk2 kinase. We demonstrate that the last 52 residues of the Smo C-term domain directly interact with the Fu regulatory domain, activating both the Fu-dependent phosphorylation of Cos2 and high levels of target gene expression. Moreover, we show that Hh-activated Smo, in tandem with Gprk2 activity, induces changes in Fu, which increase the proximity of the Fu catalytic domain and the C-term domain of Cos2, ultimately leading to the phosphorylation of S931 of Cos2.

Several publications have demonstrated that a differential magnitude of Hh signal is translated by the successive phosphorylation of Smo, a process involving several kinases including PKA, Casein kinase Iα (CkIα), CkI (Gilgamesh), CkIIα/β, protein kinase C (PKC), Fu and Gprk2 (Zhang et al., 2004; Jia et al., 2004; Zhou et al., 2006; Jia et al., 2010; Jiang et al., 2014; Li et al., 2016; Chen et al., 2010; Maier et al., 2014; Apionishev et al., 2005; Sanial et al., 2017). How the phosphorylation of Smo is converted into differential activation levels of the downstream pathway remains enigmatic. The

phosphorylation of Smo was observed in two different clusters, aa 667-746 and aa 916-1036. It has been shown that phosphorylation (by the PKA/CkI kinases) in the first cluster promotes the transition of the Smo cytoplasmic tail to an open and active conformation (Zhao et al., 2007). Phosphorylation in the second cluster by Gprk2 and Fu, which overlaps with the Fu binding site, is dependent upon the phosphorylation state of the first cluster and leads to an enhancement of Smo activity. Newly identified Fu-dependent phosphosites in the second cluster suggest the presence of a positive-feedback loop between Smo and the downstream Fu kinase (Sanial et al., 2017). Interestingly, the kinase activity of Fu is reduced when the Gprk2-dependent phosphorylation of Smo on the second cluster is blocked (Fig. 4F-I). It is thus possible that the change in electrostatic charge of the second cluster of Smo induces a conformational change, which could increase its interaction and/or accessibility to Fu and regulate the highest level of this kinase.

The question still stands as to the nature of the mechanism through which the Fu kinase interprets the different states of Smo. Here, we present new *in vitro* and *in vivo* evidence for the direct regulation of Fu by the Smo tail. As the very last amino acids of the Smo cytoplasmic tail directly interact with the Fu regulatory domain (Malpel et al., 2007; Fig. S2E), promote Fu kinase activity (Fig. 2E-F′, Fig. S2F) and are necessary for the full activation of Smo (Sanial et al., 2017), we believe that this association is important for the regulation of the catalytic activity of Fu. In contrast, the SmoΔFu variant promotes a weak Fu activity and a loss of S931 phosphorylation, and could not fully compensate for the absence of endogenous Smo (Fig. 2G-H′,J-L). SmoΔFu is still sufficient to induce the phosphorylation of serine 572 on Cos2 (Fig. S3A-C′) and induces an ectopic activation of *ptc* to a level which is lower than that at the A/P boundary (Fig. 1K; Malpel et al., 2007), confirming that the transduction complex is not fully activated by SmoΔFu. We propose that the expression of SmoΔFu leads to an overall increase in Smo, which has been shown to outcompete Ci for association with PKA and to strongly increase the level of full-length Ci (Fig. 2G′) (Ranieri et al., 2014). A similar increase in Ci is observed upon expression of a dominant-negative form of Smo, suggesting that Smo activation is not required to observe such a Ci pattern. The increase in Ci is likely to be responsible for the weak increase in Ptc and En presented in Malpel et al., 2007.

Altogether, our data suggest that Smo activates Fu in a two-step process: Fu is initially primed through its binding to the Smo residues not present in the Smo^{Fu} peptide and is subsequently activated by Smo residues present in the Smo^{Fu} peptide (Fig. 8E). We propose that, at low levels of Hh signaling, Smo activation promotes the association of Smo with Fu, independently of the last residues in the Smo C-term domain. Consequently, a conformational change in Fu is induced, increasing the proximity of Fu-Cat with Cos2, promoting the phosphorylation of Cos2 on Ser572 (Fig. 8A) and leading to the first level of Fu activation (FuAct1 in Fig. 8E). At a high level of Hh signaling, the conformational change to the Smo C-term domain is reinforced by Gprk2-dependent phosphorylation, resulting in a direct interaction between the very last amino acids of the Smo cytoplasmic tail and Fu-Reg. This interaction further enhances Fu activity (FuAct2 in Fig. 8E) and Fu-Cat proximity to Cos2, promoting phosphorylation of Ser931 (Fig. 8A). A similar influence of Gprk2 was observed in the wing imaginal discs in which we observed an Hh signaling-dependent gradient in the strength of the Smo-C-term and Fu-N-term association (Fig. 6A). This gradient is visible in the domain under the influence of Hh, and is also modulated by Gprk2 (Fig. 6F). Altogether, our results suggest that Hh signaling promotes the association of Smo C-term with Fu and changes the association of Fu

DEVELOPMENT

12

with Cos2 (Figs 5C-F‴ and 8A), leading to the final change in the phosphorylation status of Cos2 (Figs 8A′ and 2A-B′, Fig. S4A-B′).

Ascano and Robbins (2004) presented a model in which Fu-Reg associates with Fu-Cat, blocking the catalytic activity of Fu in the absence of the Hh signal. They also proposed that, upon Hh activation, the two domains dissociate and release the inhibition of Fu catalytic function. In this model, the binding of Smo to the regulatory domain of Fu would trigger the release of the Fu catalytic domain. Our data do not support this hypothesis. Indeed, we show that the interaction between both the Fu domains is constitutive in both induced and noninduced cells, and no competition was observed between Smo and the Fu catalytic domain for binding to the Fu regulatory domain (Fig. 7E, Fig. S6D). We also showed that this association is necessary to bring Fu targets, such as Fu-Reg or Cos2, within proximity of Fu-Cat in order to be phosphorylated (Figs 7C,D and 8A). As the Fu regulatory domain interacts not only with Cos2 but also with several proteins including Sufu and Smo (Monnier et al., 1998; Malpel et al., 2007; Robbins et al., 1997), we propose that it acts as a scaffold in order to bring the different substrates of Fu into the vicinity of the catalytic domain.

In this study, we also identified a complex pattern of Smo association with Fu, which follows differential levels of Hh signaling. The Smo-C-term/Fu-N-term association at high levels of Hh signaling in P cells is higher than that in A cells. Surprisingly, at high levels of Hh signaling in A cells, this association is strongly reduced, likely due to the presence of elevated Ptc (Fig. 6A). What could be the cause of the decrease in BiFC at the A/P border? It is important to note that both A cells at the A/P border and P cells display a high level of Hh signaling indicated by high levels of Smo, phosphorylated Smo and Cos2 p931 (Ranieri et al., 2012; 2014). As Ptc is not expressed in P cells, we found the pattern of BiFC intriguing and counterintuitive. It is important to note that at the A/P border, Ptc is highly expressed, but its state of activity in these cells is unknown, as there is more Ptc but also more Hh to inactivate it. The ratio of liganded to unliganded Ptc in these cells is not known. It is therefore possible that a population of unliganded Ptc is responsible for the decrease of BiFC signal and acts negatively on the Smo/Fu association. Unliganded Ptc might induce the internalization of the Smo/Fu complex in an acidic subcellular compartment, leading to a decrease in fluorescence emitted from the reconstituted YFP. We analyzed the subcellular distribution of tagged Smo and Fu in these cells and, surprisingly, did not find any significant differences in their distribution between A and P cells (data not shown). Further analysis will be necessary to resolve this issue.

MATERIALS AND METHODS
Key resources
Information on the reagents and resources used in this study is provided in Table S1.

Experimental model and subject details
Drosophila genetics
Transgenic flies (D. melanogaster) were as follows: UAS-Smo-N-YFP (Ranieri et al., 2014), UAS-C-YFP-Fu-KD; UAS-C-YFP-Fu-WT; UAS-C-YFP-Fu-EE; UAS-SmoΔFu (Malpel et al., 2007), UAS-Smo^{Fu}, UAS-Smo^{Cyto}, UAS-Smo$^{SAID-Fu}$, gprk2 KO (Cheng et al., 2010), UAS-Smo SD123, UAS-Smo GPSA (Chen et al., 2010) and UAS-DsRNA Smo 3′UTR (Maier et al., 2014). UAS transgenic flies for expression of YFP fusion protein or for Smo deletion variants were obtained by germline transformation using the phi31-intergrase into the landing site 68E1 (chromosome 3L) or 58A3 (chromosome 2R) (BestGene). The UAS-Smo dsRNA, UAS-Gprk2 dsRNA lines were obtained from the Vienna Drosophila RNAi Center. The w1118, apterous-Gal4 (ap-Gal4), rotund-Gal4 (rn-Gal4) and UAS-Dicer2 lines were

provided by the Bloomington Drosophila Stock Center. The Fu-KD is an inactive version of the Fu kinase with a substitution of Gly13 by Val in the ATP-binding site (Raisin et al., 2010). The Fu-EE construct expresses a constitutively activated Fu kinase (Zhou and Kalderon, 2011). In different genetic backgrounds, the wing imaginal discs were dissected out for immunostaining.

Drosophila cell culture
S2R+ cells were maintained in Schneider medium (Gibco) supplemented with 10% fetal bovine serum, penicillin and streptomycin. S2R+ cells were cultured and transfected for immunostaining, immunoprecipitation (IP) and western blotting (WB).

Immunostaining and microscopy
Wing imaginal discs were dissected out and fixed with 4% paraformaldehyde (PFA) in PBS (Ranieri et al., 2012). S2R+ cells grown in culture were fixed with 4% PFA in PBS for 20 min at 4°C and then washed with PBS. Discs or fixed cells were permeabilized with 0.1% Triton X-100, incubated with primary antibodies overnight at 4°C (details on primary antibodies and their dilutions are provided in Table S1), followed by secondary antibodies at room temperature for 2 h. Secondary antibodies coupled to fluorescent Alexa Fluor 405, 488, 568 and 647 (Molecular Probes) were used at a dilution of 1:400.

Images were captured with a Leica TCS SP5 confocal microscope and analyzed with ImageJ software (National Institutes of Health). To quantify fluorescence complementation, cells were transfected with plasmids encoding the two fusion proteins, and immunostained for Myc-N-YFP and HA-C-YFP using anti-HA and anti-Myc antibodies. The relative ratio of YFP fluorescence gave a measure of the relative efficiency of the complex formation. For wing imaginal discs, plots and quantifications were analyzed as described by Raisin et al. (2010).

Cell culture, transfections and DNA constructs
S2R+ cells were maintained as described in Ruel et al. (2007). Treatment with okadaic acid (OA) is described in Ruel et al. (2007). To construct the different mutant forms of Smo (Smo^{ΔSAID}, Smo^{Fu} and Smo^{Cyto}), complementary DNA fragments with Smo coding sequences at amino acid position 555-1036 (Smo^{Cyto}), 818-1036 (Smo^{ΔSAID}) and 985-1036 (Smo^{Fu}) were amplified by PCR and cloned using Gateway technology (Invitrogen) in pUAST-Myc in-frame with the Myc epitope. For expression in S2R+ cells, Smo, Fu, Gprk2 and Cos2 coding regions were inserted into the pUAST-BiFC vectors that have been described by Gohl et al., 2010. The following constructs were described in Ranieri et al. (2014): Smo-WT-Myc, Smo-AAA-Myc, Fu-WT-HA, Fu-KD-HA, Fu-WT-Myc and Cos2-Myc. For various 'tag' constructs, PKA, Fu, Cos2, Gprk2 and Smo were amplified by PCR and cloned by Gateway technology (Invitrogen) in different pUAST vectors from Carnegie Institution for Science.

The sequences of the dsDNAs used are described at http://www.flyrnai.org/. RNAi was produced in vitro from PCR products, using T7 polymerase. RNAi transfection into S2R+ cells was performed as previously described (Ruel et al., 2007).

For transient gene expression, the corresponding UAS constructs were co-transfected with an actin5C-Gal4 (Act-Gal4) construct in S2R+ cells. Transfections were carried out using Lipofectamine LTX (Invitrogen). For a total of 2 μg DNA, 50 ng to 0.2 μg DNA for each expression vector, with 1 μg Act-Gal4, was used in a typical transfection using 10 μl Lipofectamine.

IP and WB analyses
For IP and WB analyses, cells were lysed 2 days after transfection in lysis buffer [20 mM Tris-HCl (pH 8), 150 mM NaCl and 1% Triton X-100] in the presence of phosphatase inhibitors (50 mM sodium fluoride and 10 mM sodium orthovanadate) and protease inhibitors. Various HA or Myc constructs were precipitated with a mouse anti-HA or anti-Myc antibody, as described previously (Ranieri et al., 2012), and immunocomplexes were resolved by SDS-PAGE. WB was performed with antibodies against Smo, Gprk2, Fu, Cos2, Ptc, HA and Myc, as described by Ranieri et al., 2012. The anti-pSer572-Cos2 and anti-pSer93-Cos2 were used at 1:250 for WB.

Quantification and statistical analysis

For *in vitro* BiFC quantification experiments, between 150 and 200 cells were analyzed by ImageJ software (Ranieri et al., 2014). For *in vivo* experiments, BiFC and quantification were also analyzed by ImageJ software. Statistical analysis of cell count assays and quantifications was performed using Excel software. Relevant information for each experiment, including *n*-values, statistical tests and reported *P*-values, are found in the legend corresponding to each figure. In all cases, *P*<0.05 is considered statistically significant.

Supplementary information

Supplementary information available online at
http://dev.biologists.org/lookup/doi/10.1242/dev.166850.supplemental

References

Aikin, R. A., Ayers, K. L. and Thérond, P. P. (2008). The role of kinases in the Hedgehog signaling pathway. *EMBO Rep.* **9**, 330-336.

Alexandre, C., Jacinto, A. and Ingham, P. W. (1996). Transcriptional activation of Hh target gene in Drosophila is mediated directly by the cubitus interruptus protein, a member of the Gli family of zinc finger DNA-binding proteins. *Genes Dev.* **10**, 2003-2013.

Apionishev, S., Katanayeva, N. M., Marks, S. A., Kalderon, D. and Tomlinson, A. (2005). Drosophila Smoothened phosphorylation sites essential for Hedgehog signal transduction. *Nat. Cell Biol.* **7**, 86-92.

Ascano, M. and Robbins, D. J. (2004). An intramolecular association between two domains of the protein kinase Fused is necessary for Hedgehog signaling. *Mol. Cell. Biol.* **24**, 10397-10405.

Athar, M., Li, C., Kim, A. L., Spiegelman, V. S. and Bickers, D. R. (2014). Sonic Hedgehog Signaling in Basal Cell Nevus Syndrome. *Cancer Res.* **74**, 4967-4975.

Aza-Blanc, P., Ramírez-Weber, F. A., Laget, M. P., Schwartz, C. and Kornberg, T. B. (1997). Proteolysis that is inhibited by hedgehog targets Cubitus interruptus protein to the nucleus and converts it to a repressor. *Cell* **89**, 1043-1053.

Briscoe, J. and Thérond, P. P. (2013). The mechanisms of Hedgehog signaling and its roles in development and disease. *Nat. Rev. Mol. Cell Biol.* **14**, 416-429.

Chen, C.-H., von Kessler, D. P., Park, W., Wang, B., Ma, Y. and Beachy, P. A. (1999). Nuclear trafficking of Cubitus interruptus in the transcriptional regulation of Hedgehog target gene expression. *Cell* **98**, 305-316.

Chen, Y., Li, S., Tong, C., Zhao, Y., Wang, B., Liu, Y. and Jiang, J. (2010). G protein-coupled receptor kinase 2 promotes high-level Hedgehog signaling by regulating the active state of Smo through kinase-dependent and kinase-independent mechanisms in Drosophila. *Genes Dev.* **24**, 2054-2067.

Cheng, S., Maier, D., Neubueser, D. and Hipfner, D. R. (2010). Regulation of Smoothened by Drosophila G-protein-coupled receptor kinases. *Dev. Biol.* **337**, 99-109.

Fan, J., Liu, Y. and Jia, J. (2012). Hh-induced Smoothened conformational switch is mediated by differential phosphorylation at its C-terminal tail in a dose- and position-dependent manner. *Dev. Biol.* **366**, 172-184.

Gohl, C., Banovic, D., Grevelhörster, A. and Bogdan, S. (2010). WAVE forms hetero- and homo-oligomeric complexes at integrin junctions in Drosophila visualized by bimolecular fluorescence complementation. *J. Biol. Chem.* **285**, 40171-40179.

Hooper, J. E. and Scott, M. P. (1989). The Drosophila patched gene encodes a putative membrane protein required for segmental patterning. *Cell* **59**, 751-765.

Jia, J., Tong, C. and Jiang, J. (2003). Smoothened transduces Hedgehog signal by physically interacting with Costal2/Fused complex through its C-terminal tail. *Genes Dev.* **17**, 2709-2720.

Jia, J., Tong, C., Wang, B., Luo, L. and Jiang, J. (2004). Hedgehog signaling activity of Smoothened requires phosphorylation by protein kinase A and casein kinase I. *Nature* **432**, 1045-1050.

Jia, J., Zhang, L., Zhang, Q., Tong, C., Wang, B., Hou, F. and Jiang, J. (2005). Phosphorylation by double-time/CKIepsilon and CKIalpha targets cubitus interruptus for Slimb/beta-TRCP-mediated proteolytic processing. *Dev. Cell* **9**, 819-830.

Jia, H., Liu, Y., Xia, R., Tong, C., Yue, T., Jiang, J. and Jia, J. (2010). Casein kinase 2 promotes Hedgehog signaling by regulating both smoothened and Cubitus interruptus. *J. Biol. Chem.* **285**, 37218-37226.

Jiang, K., Liu, Y., Fan, J., Epperly, G., Gao, T., Jiang, J. and Jia, J. (2014). Hedgehog-regulated atypical PKC promotes phosphorylation and activation of Smoothened and Cubitus interruptus in *Drosophila*. *Proc. Natl Acad. Sci. USA* **111**, E4842-E4850.

Jiang, K., Liu, Y., Fan, J., Zhang, J., Li, X.-A., Evers, B. M., Zhu, H. and Jia, J. (2016). PI(4)P promotes phosphorylation and conformational change of smoothened through interaction with its C-terminal tail. *PLoS Biol.* **14**, e1002375.

Li, S., Chen, Y., Shi, Q., Yue, T., Wang, B. and Jiang, J. (2012). Hedgehog-regulated ubiquitination controls smoothened trafficking and cell surface expression in Drosophila. *PLoS Biol.* **10**, 1-15.

Li, S., Ma, G., Wang, B. and Jiang, J. (2014). Hedgehog induces formation of PKA-Smoothened complexes to promote Smoothened phosphorylation and pathway activation. *Sci. Signal.* **23**, 1079-1084.

Li, S., Li, S., Han, Y., Tong, C., Wang, B., Chen, Y. and Jiang, J. (2016). Regulation of Smoothened phosphorylation and high-Level Hedgehog signaling activity by a plasma membrane associated kinase. *PLoS Biol.* **14**, 1-24.

Lum, L., Zhang, C., Oh, S., Mann, R. K., von Kessler, D. P., Taipale, J., Weis-Garcia, F., Gong, R., Wang, B. and Beachy, P. A. (2003). Hedgehog signal transduction via Smoothened association with a cytoplasmic complex scaffolded by the atypical kinesin, Costal-2. *Mol. Cell* **12**, 1261-1274.

Maier, D., Cheng, S., Faubert, D. and Hipfner, D. R. (2014). A broadly conserved g-protein-coupled receptor kinase phosphorylation mechanism controls Drosophila smoothened activity. *PLoS Genet.* **10**, e1004399.

Malpel, S., Claret, S., Sanial, M., Brigui, A., Piolot, T., Daviet, L. and Plessis, A. (2007). The last 59 amino acids of Smoothened cytoplasmic tail directly bind the protein kinase Fused and negatively regulate the Hedgehog pathway. *Dev. Biol.* **303**, 121-133.

Méthot, N. and Basler, K. (1999). Hedgehog controls limb development by regulating the activities of distinct transcriptional activator and repressor forms of Cubitus interruptus. *Cell* **96**, 819-831.

Molnar, C., Holguin, H., Mayor, F., Ruiz-Gomez, A. and de Celis, J. F. (2007). The G protein-coupled receptor regulatory kinase GPRK2 participates in Hedgehog signaling in Drosophila. *Proc. Nat. Acad. Sci. USA* **104**, 7963-7968.

Monnier, V., Dussillol, F., Alves, G., Lamour-Isnard, C. and Plessis, A. (1998). Suppressor of fused links Fused and Cubitus interruptus on the Hedgehog signaling pathway. *Curr. Biol.* **8**, 583-586.

Motzny, C. K. and Holmgren, R. (1995). The Drosophila cubitus interruptus protein and its role in the wingless and hedgehog signal transduction pathways. *Mech. Dev.* **52**:137-150.

Nakano, Y., Guerrero, I., Hidalgo, A., Taylor, A., Whittle, J. R. and Ingham, P. W. (1989). A protein with several possible membrane-spanning domains encoded by the Drosophila segment polarity gene patched. *Nature* **341**, 508-513.

Nybakken, K. E., Turck, C. W., Robbins, D. J. and Bishop, M. J. (2002). Hedgehog-stimulated phosphorylation of the kinesin-related protein Costal2 is mediated by the serine/threonine kinase Fused. *J. Biol. Chem.* **277**, 24638-24647.

Ogden, S. K., Ascano, J. M., Stegman, M. A., Suber, L. M., Hooper, J. E. and Robbins, D. J. (2003). Identification of a functional interaction between the transmembrane protein smoothened and the kinesin-related protein costal2. *Curr. Biol.* **11**, 1998-2003.

Préat, T., Thérond, P., Lamour-Isnard, C., Limbourg-bouchon, B., Tricoire, H., Erk, I., Mariol, M. C. and Busson, D. (1990). A putative serine/Threonine protein kinase encoded by the segment-polarity fused gene of Drosophila. *Nature* **374**, 87-89.

Price, M. A. and Kalderon, D. (2002). Proteolysis of the Hedgehog signaling effector Cubitus interruptus requires phosphorylation by Glycogen Synthase Kinase 3 and Casein Kinase 1. *Cell* **108**, 823-835.

Raisin, S., Ruel, L., Ranieri, N., Staccini-Lavenant, L. and Thérond, P. P. (2010). Dynamic phosphorylation of the kinesin Costal-2 *in vivo* reveals requirement of Fused kinase activity for all levels of hedgehog signaling. *Dev. Biol.* **344**, 119-128.

Ranieri, N., Ruel, L., Gallet, A., Raisin, S. and Thérond, P. P. (2012). Distinct phosphorylations on kinesin Costal-2 mediate differential Hedgehog signaling strength. *Dev. Cell* **22**, 279-294.

Ranieri, N., Thérond, P. P. and Ruel, L. (2014). Switch of PKA substrates from Cubitus interruptus to Smoothened in the Hedgehog signalosome complex. *Nat. Commun.* **5**, 5034.

Robbins, D. J., Nybakken, K. E., Kobayashi, R., Sisson, J. C., Bishop, J. M. and Thérond, P. P. (1997). Hedgehog elicits signal transduction by means of a large complex containing the kinesin-related protein Costal2. *Cell* **90**, 225-234.

Robbins, D. J., Fei, D. L. and Riobo, N. A. (2012). The Hedgehog signal transduction network. *Sci. Signal.* **5**, re6.

Ruel, L., Rodriguez, R., Gallet, A., Lavenant-Staccini, L. and Thérond, P. P. (2003). Stability and association of Smoothened, Costal2 and Fused with Cubitus interruptus are regulated by Hedgehog. *Nat. Cell Biol.* **5**, 907-913.

Ruel, L., Gallet, A., Raisin, S., Truchi, A., Staccini-Lavenant, L., Cervantes, A. and Thérond, P. P. (2007). Phosphorylation of the atypical kinesin Costal2 by the kinase Fused induces the partial disassembly of the Smoothened-Fused-Costal2-Cubitus interruptus complex in Hedgehog signaling. *Development* **134**, 3677-3689.

Sanial, M., Bécam, I., Hofmann, L., Behague, J., Argüelles, C., Gourhand, V., Bruzzone, L., Holmgren, R. A. and Plessis, A. (2017). Dose-dependent transduction of Hedgehog relies on phosphorylation-based feedback between the G-protein-coupled receptor Smoothened and the kinase Fused. *Development* **144**:1841-1850.

Scales, S. J. and de Sauvage, F. J. (2009). Mechanisms of Hedgehog pathway activation in cancer and implications for therapy. *Trends Pharmacol. Sci.* **30**, 303-312.

Shi, Q., Li, S., Jia, J. and Jiang, J. (2011). The Hedgehog-induced Smoothened conformational switch assembles a signaling complex that activates Fused by promoting its dimerization and phosphorylation. *Development* **138**, 4219-4231.

Shyu, Y. J. and Hu, C. D. (2008). Fluorescence complementation: an emerging tool for biological research. *Trends Biotechnol.* **26**, 622-630.

Sisson, J. C., Ho, K. S., Suyama, K. and Scott, M. P. (1997). Costal2, a novel kinesin related protein in the Hedgehog signaling pathway. *Cell* **90**, 235-245.

Smelkinson, M. G. and Kalderon, D. (2006). Processing of the Drosophila Hedgehog signaling effector Ci-155 to the repressor Ci-75 is mediated by direct binding to the SCF component Slimb. *Curr. Biol.* **16**, 110-116.

Smelkinson, M. G., Zhou, Q. and Kalderon, D. (2007). Regulation of Ci-SCFSlimb binding, Ci proteolysis, and Hedgehog pathway activity by Ci phosphorylation. *Dev. Cell* **13**, 481-495.

Tian, L., Holmgren, R. A. and Matouschek, A. (2005). A conserved processing mechanism regulates the activity of transcription factors Cubitus interruptus and NF-kappaB. *Nat. Struct. Mol. Biol.* **12**, 1045-1053.

Wang, Q. T. and Holmgren, R. A. (1999). The subcellular localization and activity of Drosophila cubitus interruptus are regulated at multiple levels. *Development* **126**, 5097-5106.

Wang, G., Amanai, K., Wang, B. and Jiang, J. (2000). Interactions with Costal2 and suppressor of fused regulate nuclear translocation and activity of cubitus interruptus. *Genes Development* **14**, 2893-2905.

Whitington, T., Jolma, A. and Taipale, J. (2011). Beyond the balance of activator and repressor. *Sci. Signal.* **4**, pe29.

Xia, R., Jia, H., Fan, J., Liu, Y. and Jia, J. (2012). USP8 promotes smoothened signaling by preventing its ubiquitination and changing its subcellular localization. *PLoS Biol.* **10**, 1-16.

Yao, S., Lum, L. and Beachy, P. (2006). The ihog cell-surface proteins bind Hedgehog and mediate pathway activation. *Cell* **125**, 343-357.

Zhang, C., Williams, E. H., Guo, Y., Lum, L. and Beachy, P. A. (2004). Extensive phosphorylation of Smoothened in Hedgehog pathway activation. *Proc. Natl. Acad. Sci. U.S.A.* **101**, 17900-17907.

Zhang, W., Zhao, Y., Tong, C., Wang, G., Wang, B., Jia, J. and Jiang, J. (2005). Hedgehog-regulated Costal2-kinase complexes control phosphorylation and proteolytic processing of Cubitus interruptus. *Dev. Cell* **8**, 267-278.

Zhang, Y., Mao, F., Lu, Y., Wu, W., Zhang, L. and Zhao, Y. (2011). Transduction of the Hedgehog signal through the dimerization of Fused and the nuclear translocation of Cubitus interruptus. *Cell Res.* **21**, 1436-1451.

Zhao, Y., Tong, C. and Jiang, J. (2007). Hedgehog regulates Smoothened activity by inducing a conformational switch. *Nature* **450**, 252-258.

Zhou, Q. and Kalderon, D. (2011). Hedgehog activates Fused through phosphorylation to elicit a full spectrum of pathway responses. *Dev. Cell* **20**, 802-814.

Zhou, Q., Apionishev, S. and Kalderon, D. (2006). The contributions of protein kinase A and smoothened phosphorylation to hedgehog signal transduction in Drosophila melanogaster. *Genetics* **173**, 2049-2062.

DEVELOPMENT